ELSEVIER

Powder Technology 120 (2001) 256–263

POWDER TECHNOLOGY

www.elsevier.com/locate/powtec

Preparation and characterization of sol–gel derived mesoporous titania spheroids

Kamal M.S. Khalil [a,*], Mohamed I. Zaki [b]

[a] *Chemistry Department, Faculty of Science, UAE University, PO Box 17551, Al-Ain, United Arab Emirates*
[b] *Chemistry Department, Faculty of Science, Kuwait University, PO Box 5969, Safat 13060, Kuwait*

Received 1 March 2000; received in revised form 1 November 2000; accepted 22 January 2001

Abstract

The formation of mesoporous spherical titania particles via hydrolysis of pure titanium tetra-isopropoxide in *n*-heptane solution upon the application of a slow stirring rate is described. Calcination of the dry hydrolysis product produced pure anatase at 400–600°C, and rutile at 800°C. Nitrogen adsorption results indicate high surface area (S_{BET} 132 m^2/g) and uniform mesopores peaking at 10 nm for the material calcined at 400°C. Upon calcination at 600°C, the pore size remained at 10 nm, whereas the S_{BET} value was decreased. The material calcined at 400°C was found by scanning electron microcopy to be shaped into spherical particles about 2 μm in diameter. Sizes of the spherical particles were unchanged at 400°C and up to 800°C. This was ascribed to the spherical morphology of the particles which prevented primary particles from growing beyond the boundary of the host aggregate even when the rutile phase transition occurred at 800°C.

Keywords: Sol–gel; Titania; Spherical particles; N_2 adsorption; SEM

1. Introduction

Preparation of porous materials with controlled formation of mesopores and high specific surface area for use as filters, adsorbents, catalysts, and catalyst supports has attracted much interest [1–8]. Since the performance of such materials is largely determined by their thermal stability, much interest has been focused on the improvement of the materials' textural and structural stability [2–4].

Sol–gel processing of metal alkoxides offers various possibilities for obtaining tailor made materials. In an effort to prepare titania powders with increasing textural and structural stability, Music et al. [6] have stabilized the colloidal suspension of titania (prepared by sol–gel processing) with polyethylene glycol to prevent sintering of titania particles during calcination of the precursor materials. Mesoporous titania with a large surface area (up to 103 m^2/g) has been prepared [9] by calcination of hybrid composites obtained by incorporation of the biopolymer Chitosan in titania networks produced from titanium isopropoxide. Another trial for the preparation of mesoporous titania was carried out by Takahashi et al. [10], whereby titania was produced from titanium isopropoxide and stearic acid.

Significant efforts have been made to control the shape and the size of titania particles prepared via alkoxides including methods based on vapour phase pyrolysis [11] or hydrolysis [12]. Synthesis of spherical titania particles by sol–gel processing of, tetraethyl orthotitanate (TEOT) have been widely investigated [13–16]. Yamashita et al. [13] obtained spherical particles by addition of diethanolamine or 2-methoxyethanol in the starting solution. Upon calcination at 500°C or 700°C, the particles were anatase or rutile phase, respectively. Selle et al. [14] prepared spherical particles, in the size range 0.5–0.8 μm, from TEOT at low temperature and concentration of ammonia up to 0.01 M. Kumazawa et al. [15] investigated the use of controlled hydrolysis of TOET in ethanol for the preparation of spherical titania particles. The use of electrolytes to control size, agglomeration levels, and spherical particle formation from TEOT has been studied by Look and Zukoski [16].

Thus, many studies have examined methods for making spherical titania particles from TEOT solutions with additives. This is probably due to the idea that: "the ideal powder should be pure, stoichiometric, dense, spheroidal,

* Corresponding author. Fax: +971-3-767-1291.
E-mail address: kamalk@uaeu.ac.ae (K.M.S. Khalil).

0032-5910/01/$ - see front matter
PII: S0032-5910(01)00278-9

and nearly monodisperse" [17]. The present paper examines the formation of mesoporous spherical titania xerogel from sol–gel processing of another alkoxide, titanium tetra-isopropoxide, $Ti(OPr^i)_4$, in *n*-heptane solvent with no additives, to assure purity. Formation, characterization, morphology, and sintering of the obtained xerogel material and its calcination products at 400–800°C are discussed.

2. Experimental

2.1. Materials

The titanium (IV) isopropoxide ,$Ti(OPr^i)_4$, used was 99.9% pure liquid (Aldrich). *n*-Heptane, C_7H_{16}, used was 99.99% (Aldrich).

The hydrolysis of the alkoxide was carried out by dropwise addition (through 1 min) of a calculated stoichiometric amount of distilled water to 600 ml of 0.4 M solution of the alkoxide in *n*-heptane. The solution was magnetically stirred at 100 rpm during the water addition, and stirred at the same rate for 1 h thereafter. The solution was aged for 3 days at room temperature, then filtered off using Whatman filter paper. The resulting gel was allowed to dry at ambient overnight, then further at 60°C for 24 h to give the xerogel material. Portions of the xerogel material were calcined for 3 h at 400°C, 600°C, and 800°C, and used as test materials.

2.2. Techniques

Thermal analysis was carried out utilizing a Thermal Analyst 2000 TA instrument (USA) controlling a 2050 thermogravimetric (TG) analyzer and a 2010 differential scanning calorimeter (DSC). A ceramic sample boat was used for TG runs. Samples weighing 10.0 ± 0.1 mg were

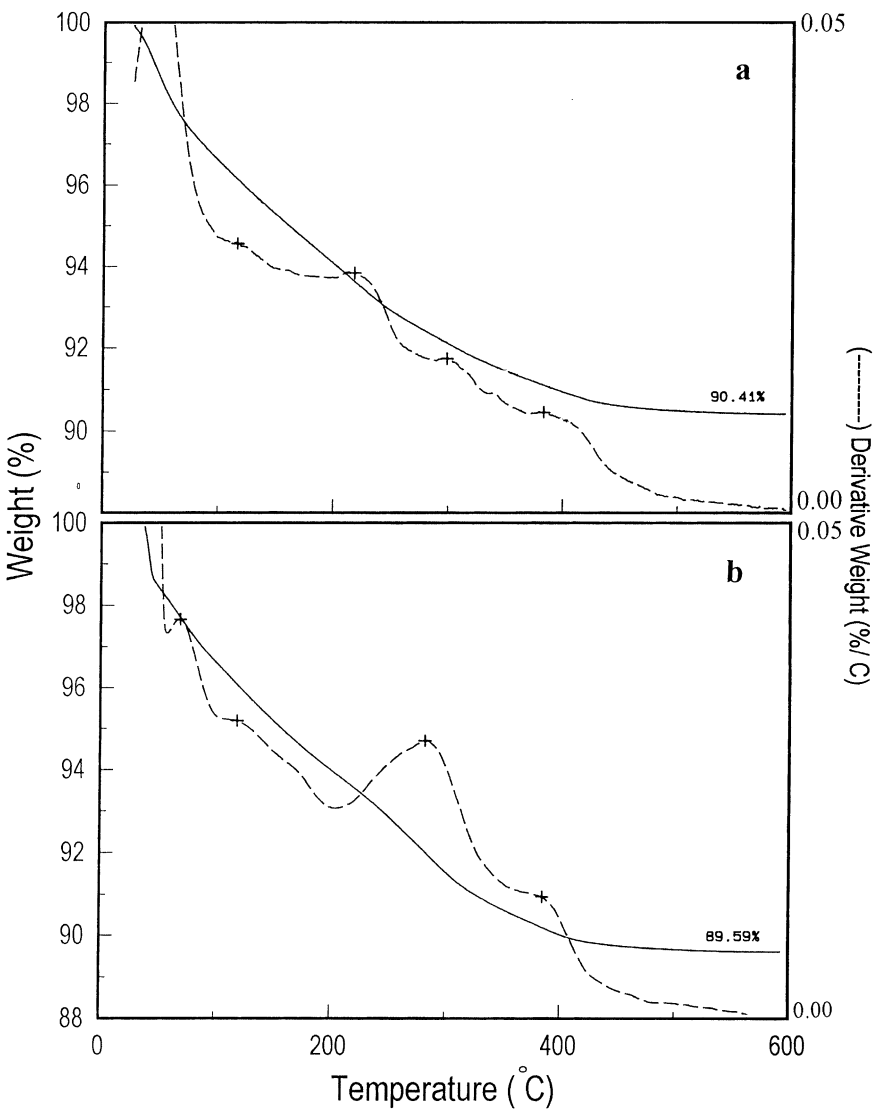

Fig. 1. TG and DTG curves recorded for the xerogel materials on heating up to 600°C at 10°C/min and 30 ml/min flow of (a) nitrogen and (b) oxygen.

heated up to 600°C at 10°C/min and in a stream (30 ml/min) of nitrogen or oxygen atmosphere. For DSC measurement, open aluminum sample pans were used. Samples weighing 5.0 ± 0.1 mg were heated up to 500°C at 10°C/min in similar dynamic atmosphere of nitrogen or oxygen.

X-ray Powder diffractometry (XRD) was carried out using a model JSX-60 PA Jeol (Japan) diffractometer equipped with Ni-filtered CuK radiation. JCPDS-ICDD standard data [18] were referred to for phase identification purposes.

N_2 gas adsorption–desorption isotherms were measured at −196°C using a model ASAP 2010 Micrometrics Instrument (USA). Test samples were thoroughly outgassed for 2 h at 160°C, prior to exposure to the adsorptive atmosphere. The specific surface area, S_{BET}, values was calculated applying the BET equation [19]. Pore volume distribution curves were generated (with the adsorption branch isotherms) by DFT plus V1.00 (2010) software of the instrument indicated, implementing the original density function theory, and adopting the slit pore shape [20].

SEM micrographs were obtained after coating of the test materials with gold, using a model 5600 Jeol (Japan) scanning electron microscope.

3. Results

TG and DTG curves recorded for the xerogel materials in nitrogen and oxygen gas atmosphere are shown in Fig. 1a and b, respectively. The curves show that the material dehydrates gradually. The total weight loss determined at 600°C was 9.61% in N_2 atmosphere, and 10.39% in oxygen gas flow.

The corresponding DSC curves shown in Fig. 2 show two endothermic peaks at ≤ 150°C, which could be related to the elimination of water and remaining organic solvent molecules [21]. A large exothermic peak was observed at 225°C in O_2 flow whereas a much smaller one was observed at 243°C in N_2 flow. These exotherms could be associated with the oxidative elimination of organic residue and/or crystallization.

XRD patterns are presented for products of the xerogel calcined at 400–800°C as shown in Fig. 3. The 400°C and 600°C calcined materials were indexed as titania assuming the anatase structure. However, the overall crystallinity largely improved for the latter calcined material. The 800°C calcined material was indexed as being rutile TiO_2.

Fig. 4 shows the N_2 adsorption–desorption isotherm of the materials calcined at 400–800°C. The isotherm of the 400°C calcined materials (Fig. 4a) is essentially of type IV being diagnostic of mesoporous materials [22]. The isotherm shows also a little rising up portion at $P/P_o > 0.90$, which reveals some properties, related to type II isotherms. The hysteresis loop exhibited is largely of type H1 with some contribution from type H2 [22].

The isotherm obtained for the 600°C calcined material (Fig. 4b) bears a great deal of similarity to the above isotherm, except for an increasing type II contribution at the expense of the type IV contribution. Noticeably, however, the total volume adsorbed near $P/P_o = 1$ was reduced. The hysteresis loop observed is also similar to that

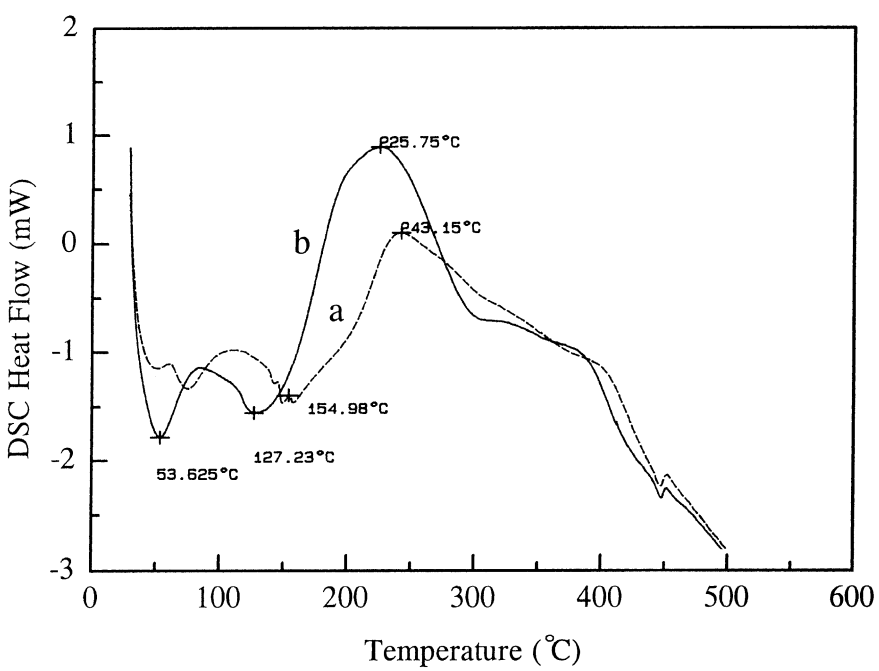

Fig. 2. DSC curves recorded for the xerogel materials on heating up to 500°C at 10°C/min and 30 ml/min flow of nitrogen (curve a) and oxygen (curve b).

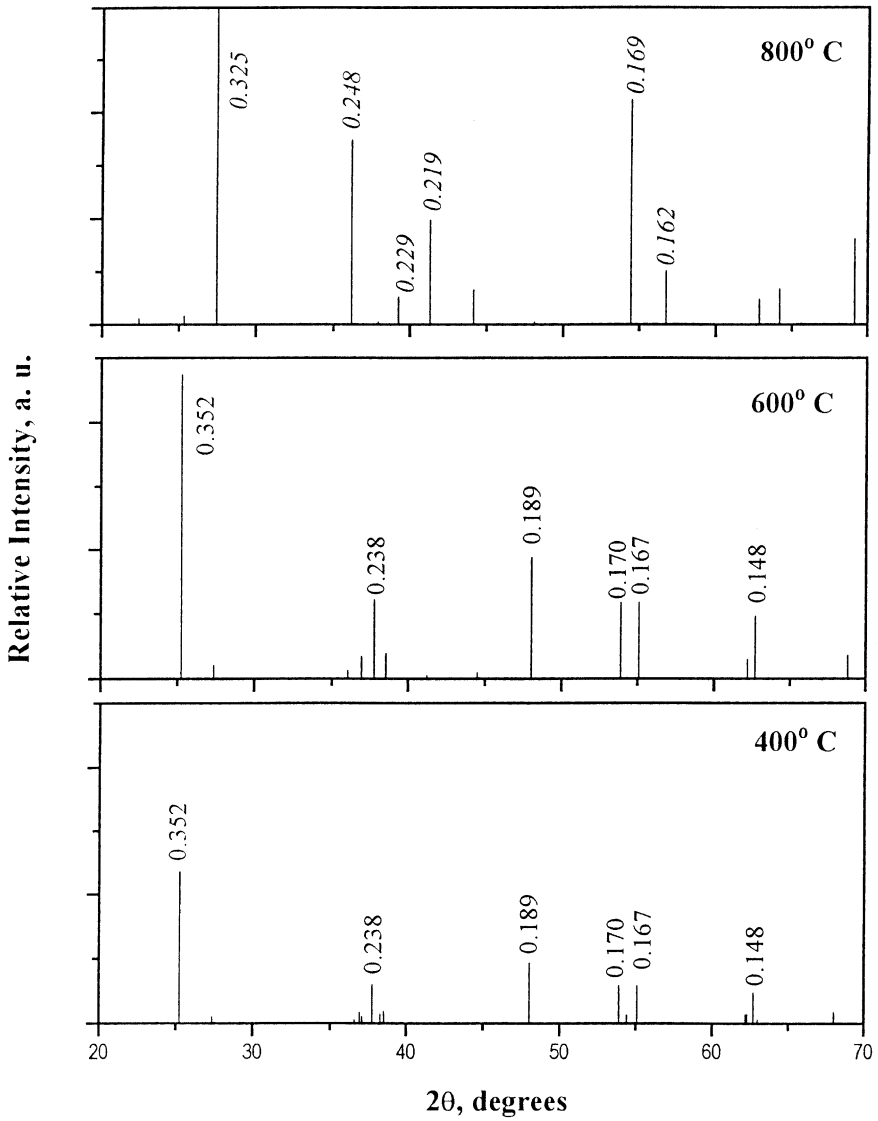

Fig. 3. XRD diffractograms for the materials calcined at 400°C, 600°C, 800°C, as indicated. *d*-Spacing values for the strongest diffraction peaks are indicated for anatase and rutile (italic) in nanometers.

observed for the 400°C calcined material (Fig. 4a). However, an increasing contribution from type H2 can be observed.

The isotherm obtained for the 800°C calcined materials (Fig. 4c) indicates a dramatic progression of the type II at the expense of the type IV. The total volume adsorbed near $P/P_o = 1$ was consistently dramatically reduced, and the hysteresis loop largely absent.

BET Surface areas determined for the calcined materials are cited in Table 1. Accordingly the 400°C calcined material had specific surface area (131.9 m^2/g) higher than that (58.5 m^2/g) of the material calcined at 600°C, and much higher than that (5.0 m^2/g) of the material calcined at 800°C.

Fig. 5 exhibits the pore volume distribution (PVD) curves obtained for the 400–800°C calcined materials of the xerogel. The PVD curve of the 400°C calcined material showed the main porosity in the pore width range 5–20 nm, sharply peaking at 10 nm. The PVD curve of the 600°C calcined material (Fig. 5) was shown to be similar to the above curve with the same peak in pore width at 10 nm. However, the distribution has been reduced over the entire range of pore width. The PVD curve of the 800°C calcined material (Fig. 5) was shown to exhibit no detectable porosity.

Particle morphology of the different calcined materials was examined by scanning electron microscopy (SEM). A typical SEM micrograph obtained for the 400°C calcined material (Fig. 6) showed the material to consist of spheroidal particles of 2 μm in size packed together. The SEM micrograph (Fig. 7) of the 600°C calcined material reflects a similar morphology to that of the 400°C calcined material. The SEM micrograph (Fig. 8) of the 800°C calcined materials shows the spherical particles still pre-

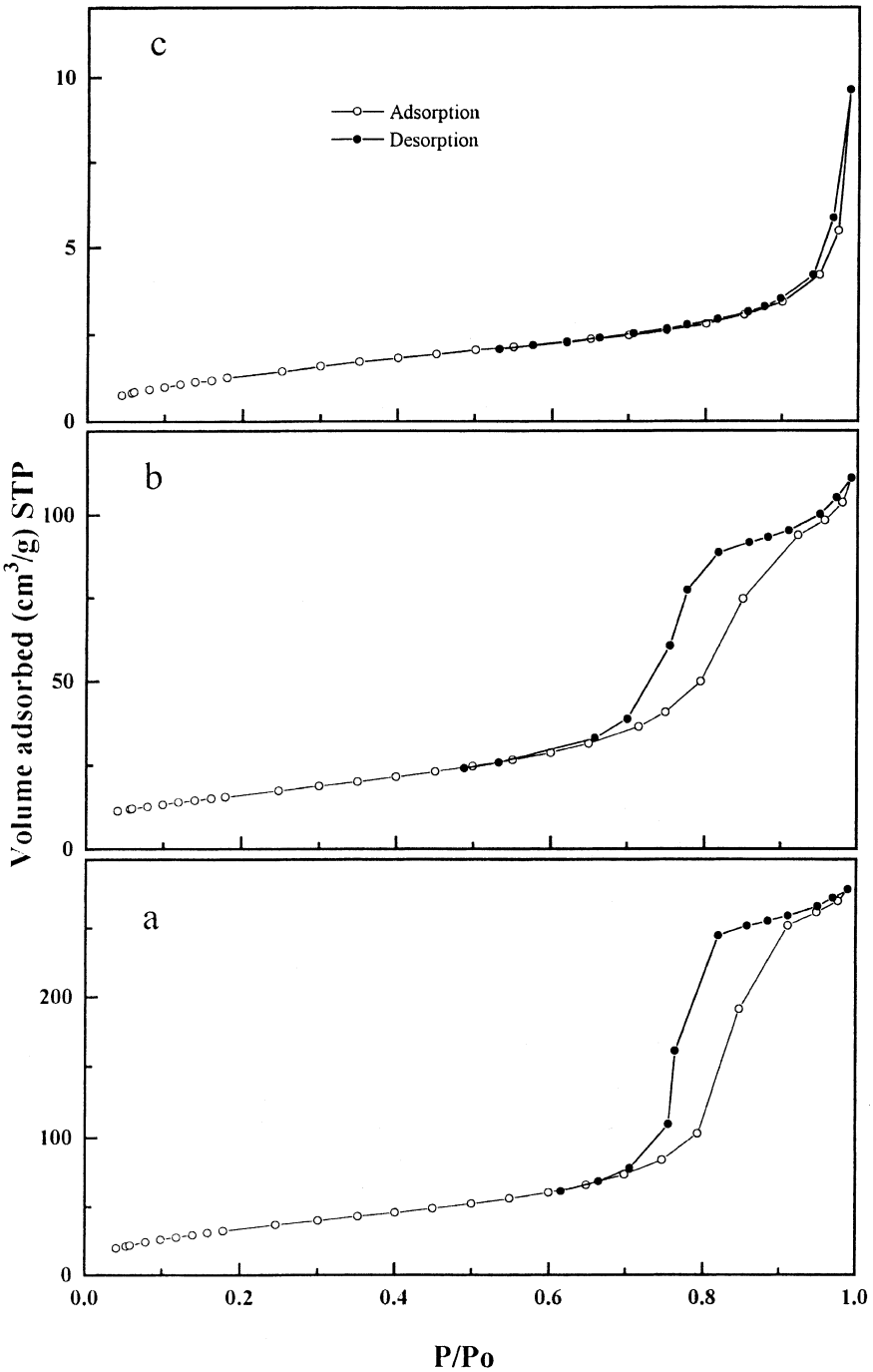

Fig. 4. N_2 adsorption/desorption isotherm of materials calcined at 400°C (a), 600°C (b), and 800°C (c).

serve their shape; nevertheless a case of slight coalescence between the spherical particles was observed. However, in all cases the particle size was limited by the size of the original spherical particles.

Table 1
BET surface area (S_{BET}) for the calcined materials

Material	S_{BET} (m^2/g)
400°C calcined	131.9 ± 1.3
600°C calcined	58.5 ± 0.4
800°C calcined	5.0 ± 0.1

4. Discussion

The present results showed that the hydrolysis of $Ti(OPr^i)_4$ in *n*-heptane media when stirred at 100 rpm led to successful formation of spherical titania particles. Previ-

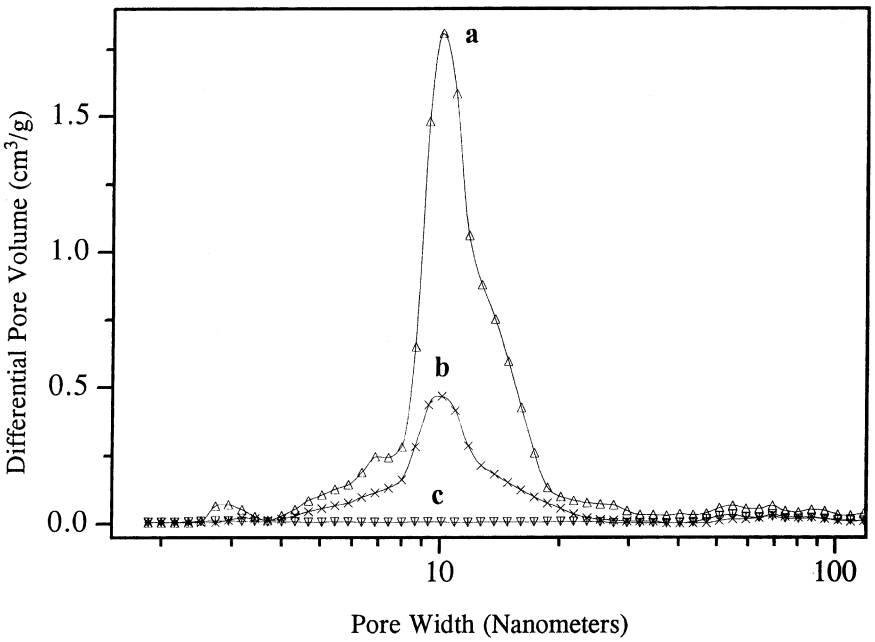

Fig. 5. Pore width distribution for the materials calcined at 400°C (a), 600°C (b), and 800°C (c).

ously, the hydrolysis of $Ti(OPr^i)_4$ in *n*-heptane under a higher stirring rate (400 rpm), as investigated by HRTEM, was shown [23] to result in the formation of ~ 10 nm primary particles. It was evident that these nanosized particles were aggregating together into agglomerates of irregular shape and submicron size. The question now is why the present slow stirring rate produces spherical particles, whereas the higher stirring rate applied previously [23] did not. In fact, Look and Zukoski [24] investigated the hydrolysis of $Ti(OEt)_4$ in aqueous ethanol solution. They found that in the presence of shear, particles initially grow as discrete units. However, above a critical shear rate the particles grew to a size at which they aggregate and the final precipitate is composed of agglomerates consisting of fused particles.

Thus, the present spherical particles are formed as a consequence of lowering of the stirring rate in *n*-heptane. The function of *n*-heptane which is an aprotic solvent may be regarded as a hydrolysis controller since the hydrolysis actually occur at the *n*-heptane/stirred water droplets interface. Then, the preferential adsorption will make the hydrolyzed species at the interface to diffuse into the water droplets. As further hydrolyzed species formed at the interface, the hydrolyzed product diffused into the water droplets. The hydrolysis of titanium alkoxides is known to lead to the formation of small particles that aggregate into secondary particles of larger size [23]. Thus, each water droplet will act as a micro reactor in which the initial small titania particles are aggregate, the natural shape of the droplets being reflected in the shape of the aggregates. As

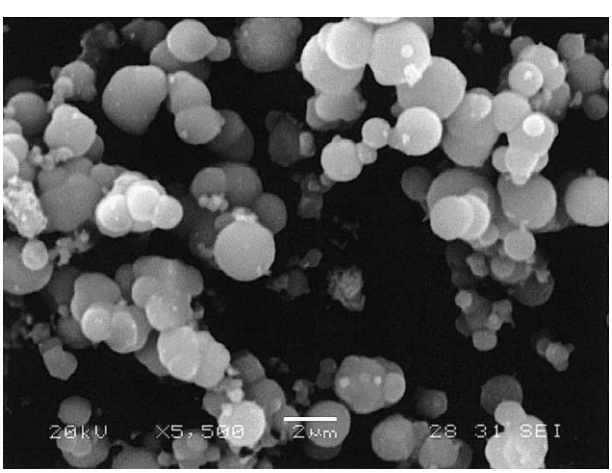

Fig. 6. SEM micrograph for titania calcined at 400°C.

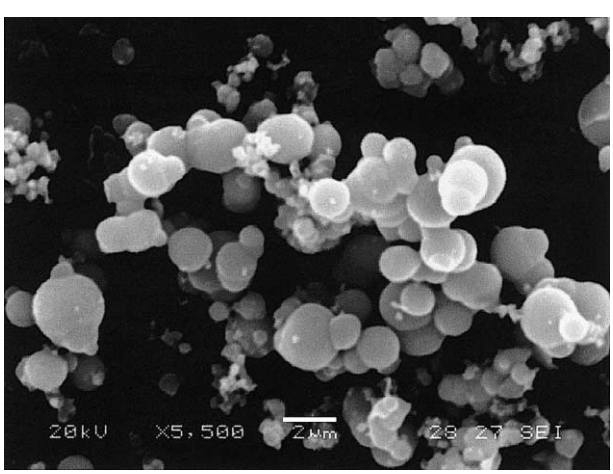

Fig. 7. SEM micrograph for titania calcined at 600°C.

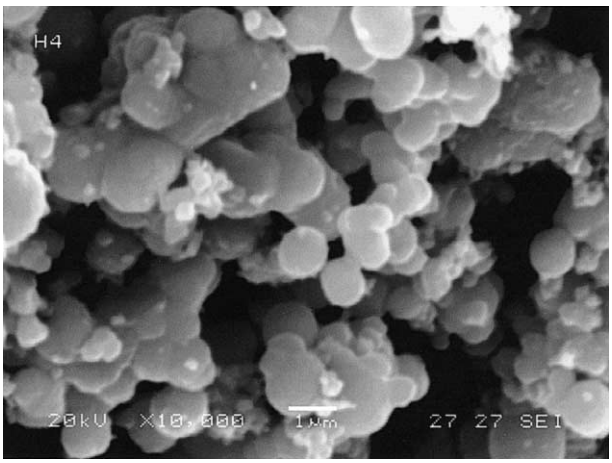

Fig. 8. SEM micrograph for titania calcined at 800°C.

long as water droplet collisions are minimized the production of spherical particle is possible. Conversely increasing the stirring rate will increase the likely collision between water droplets, causing coalescence with the production of irregular aggregates.

The observation of the 400–800°C calcined titania particles in the form of spheres indicates that they retained the spherical shape of the original hydrous aggregates. The low crystallinity of the 400°C material (see the relative intensity of the different crystalline materials in Fig. 3) indicates the presence of many amorphous and/or small size particles. Probably, the presence of organic residues in the dried hydrolysis products, as shown by DSC results, could protect the small grains from coalescence, i.e. preventing their growth and giving rise to microcrystalline grains.

N_2 adsorption isotherms confirm the above prediction. The isotherm of the 400°C calcined materials (type IV) indicates mesoporous materials [22]. However, the observed contribution from type II isotherms, indicate some properties of macro-porous (or non-porous) solids [22]. The hysteresis loop observed with the isotherm was mainly of type H1, which characterizes agglomerates of approximately uniform size giving rise to a narrow pore size distribution. Moreover, the contribution from type H2 loop indicates networking porosity [22]. The isotherms obtained for the 600°C calcined material (Fig. 4b) indicates that the material has got less mesoporosity than the materials calcined at 400°C. The dramatic progression of the type II for the isotherm obtained for the 800°C calcined material (Fig. 4c) accounts for a macroporous (or non-porous) material.

Calcination at 600°C resulted in the decrease of surface area from ca. 132 to 59 m^2/g. Moreover, crystallinity of the material was improved, and a well crystalline anatase was formed. Calcination at 800°C resulted in structural transformation into rutile phase. At this stage particle growth beyond the aggregate limits was scarcely observed.

The above information derived from gas adsorption–desorption isotherms can be treated adequately on the basis of particle-packing models [7,25,26]. Accordingly, formation of a hierarchical microstructure in which fully dense particles are randomly close-packed into agglomerates that are in turn randomly close packed, may be supposed. For models based on backing of spheres, the type of packing, and extent of aggregation effectively determine the xerogel porosity. The effect of aggregation is basically an increase in the pore diameter that corresponds to a given particle size. Thus, the present observation that the pore size ($\sim$ 10 nm) remained unchanged upon increasing of the calcination temperature from 400°C to 600°C indicates that no aggregation for the initial particles occurred. However, the reduction of the surface area could presumably be due to neck formation and/or narrowing of pore interance [7,27].

Thus, the present results are in line with those reported by Hague and Mayo [28] who studied the effect of crystallization and phase transformation on the grain growth of TiO_2. They found, during sintering that the presence of inter-agglomerate pores served to prevent individual anatase grains from growing beyond the boundary of the host agglomerate.

5. Conclusions

Spherical titania xerogel is formed via sol–gel processing of $Ti(OPr^i)_4$ in *n*-heptane solvent (with no additives) upon stirring at 100 rpm. It is assumed that each water droplet may act as a micro reactor in which initial titania particles aggregates. The spherical shape of the aggregates is considered as a reflection of the water droplets' shape. The stirring rate is a crucial processing parameter, since a higher stirring rate (400 rpm) was found previously [23] to produce irregular aggregates. A thorough investigation of the effect of stirring rate and water droplet size on the final morphology of the xerogel particles is worth attempting.

The hierarchical microstructure is supposed for, the high surface area and uniform mesopores, 400°C calcined materials. Moreover, pore size uniformity (at 10 nm) is unchanged upon increasing of the calcination temperature to 600°C.

References

[1] K.M.S. Khalil, M.I. Zaki, Powder Technol. 92 (1997) 233.
[2] C.L. Murrel, Catal. Today 35 (1997) 225.
[3] D.L. Trimm, Design of Industrial Catalysts, Oxford Univ. Press, New York, 1984.
[4] K.M.S. Khalil, J. Catal. 178 (1998) 198.
[5] G.M. Pajonk, Catal. Today 35 (1997) 319.
[6] S. Music, M. Gotic, M. Ivanda, S. Popovic, A. Turkovic, R. Trojko, A. Sekulic, K. Furic, Mater. Sci. Eng., B 47 (1997) 33.
[7] D.J. Suh, T.-J. Park, Chem. Mater. 8 (1996) 509.
[8] T. Lopez, E. Sanchez, P. Bosch, Y. Meas, R. Gomez, Mater. Chem. Phys. 32 (1992) 141.
[9] J. Retuert, R. Quijada, V. Arias, Chem. Mater. 10 (1998) 3923.

[10] R. Takahashi, S. Takenaka, S. Sato, T. Sodesawa, K. Ogura, K. Nakanishi, J. Chem. Soc., Faraday Trans. 94 (1998) 3161.
[11] K.M.S. Khalil, M.I. Zaki, A.A. ElSamahy, J. Anal. Appl. Pyrolysis 42 (1997) 123.
[12] J. Rubio, J.L. Oteo, M. Villegas, P. Duran, J. Mater. Sci 32 (1997) 643.
[13] H. Yamashita, K. Nozaki, K. Toshinari, T. Mima, T. Maekawa, J. Ceram. Soc. Jpn. 106 (1998) 1184.
[14] M.H. Selle, J. Sjoeblom, R. Lindberg, Colloid Polym. Sci. 273 (1995) 951.
[15] H. Kumazawa, H. Otsuki, E. Sada, J. Mater. Sci. Lett. 12 (1993) 839.
[16] J.L Look, C.F. Zukoski, J. Am. Chem. Soc. 75 (1992) 1587.
[17] C.J. Brinker, G.W. Scherer, Sol–Gel Science, The Physics and Chemistry of Sol–Gel Processing, Academic Press, New York, 1989, p. 722.
[18] JCPDS, International Center for Diffraction Data, CD, 1996.
[19] B. Brunaure, P.H. Emmett, E. Teller, J. Am. Chem. Soc. 60 (1938) 309.
[20] Micrometrics DFT Plus, V1.00, Operator's Manual, 1996.
[21] D. Terribile, A. Trovarelli, J. Llorca, C. de Leitenburg, G. Dolcetti, J. Catal. 178 (1998) 299.
[22] International Union of Pure and Applied Chemistry (IUPAC), Pure Appl. Chem. 57 (1985) 603.
[23] K.M.S. Khalil, T. Baird, M.I. Zaki, A.A. El-Samahy, I.M. Awad, Colloids Surf., A 132 (1998) 31.
[24] J.-L. Look, C.F. Zukoski, J. Colloid Interface Sci. 153 (1992) 461.
[25] J.D.F. Ramsay, R.G. Avery, Br. Ceram. Proc. 38 (1986) 275.
[26] C.J. Brinker, G.W. Scherer, J. Non-Cryst. Solids 70 (1985) 301.
[27] S.J. Greeg, K.S.W. Sing, Adsorption Surface Area and Porosity, Academic Press, London, 1982.
[28] D.C. Hague, M.J. Mayo, Nanostruct. Mater 3 (1993) 61.